

2007

The Shape of Pulverized Bituminous Vitrinite Coal Particles

Jonathan P. Mathews

Patrick G. Hatcher

Old Dominion University, phatcher@odu.edu

Alan W. Scaroni

Follow this and additional works at: https://digitalcommons.odu.edu/chemistry_fac_pubs

 Part of the [Chemical Engineering Commons](#), and the [Materials Chemistry Commons](#)

Repository Citation

Mathews, Jonathan P.; Hatcher, Patrick G.; and Scaroni, Alan W., "The Shape of Pulverized Bituminous Vitrinite Coal Particles" (2007). *Chemistry & Biochemistry Faculty Publications*. 3.
https://digitalcommons.odu.edu/chemistry_fac_pubs/3

Original Publication Citation

Mathews, J.P., Eser, S., & Hatcher, P.G. (2007). The shape of pulverized bituminous vitrinite coal particles. *Kona-Powder and Particle*, 25, 145-152.

The Shape of Pulverized Bituminous Vitrinite Coal Particles[†]

Jonathan P. Mathews*, Semih Eser,
Energy Institute and Department of Energy & Mineral
Engineering, The Pennsylvania State University¹

Patrick G. Hatcher,
Department of Chemistry & Biochemistry, Old Dominion
University²

Alan W. Scaroni
Energy Institute and Department of Energy & Mineral
Engineering, The Pennsylvania State University¹

Abstract

The shape of pulverized bituminous coal particles (vitrinites) was determined by optical and laser light scattering. Vitrinite samples were collected from obvious tree remains located in the ceilings of two Appalachian coal mines. Wet sieving produced narrow size cuts. The particles were determined to be oblong or blocky in shape, with average length-to-width ratio of 1.7 and sphericity of 0.78. They were analogous in shape to a square ended, rectangular "house brick". The two bituminous coals and different size cuts of each coal had essentially the same shape parameters. Characteristic heating times and terminal velocities were higher by 22 and 20%, respectively compared to spherical particles.

Keywords: Coal particle shape

1. Introduction

The size and shape of coal particles influence their heat and mass transfer characteristics, behavior in fluids, erosion potential, and inhalation-related health risks¹⁻⁴. Unfortunately, the exiguous information that is available on the shape of coal particles has often been inferred from indirect techniques⁵. Coal is a complex organic solid. The chemical and physical composition is influenced by the organic and inorganic precursors, deposition environment, and burial history. The macerals (those components of coals identifiable under the microscope as organic and identified based upon morphology and reflectance), which emanate from diverse biomass precursors also possess characteristic sizes, shapes and friabilities and thus tend to concentrate in different size fractions⁶⁻¹¹. Hence, maceral composition has the potential to affect shape parameters of size fractions.

Advanced separation techniques can produce high purity maceral concentrates¹² but only in particle sizes far smaller than those found in conventional pulverized coal. In addition, extensive milling is likely to produce increasingly spherical particles.

North American coals tend to be rich in vitrinite. The average vitrinite content of the 878 samples in the Penn State Coal Sample Bank is 75% (based on an ASTM point counting technique)¹³. In this work the influence of other macerals was minimized by sampling obvious coalified trees that were monomaceral (telocollinite) in composition. Digital image analysis of reflectance microscopy images (along with SEM micrographs) provided direct observation of particle shape and allowed mineral matter to be excluded from the statistical analysis.

2. Experimental

The vitrinite samples were collected from Sigillaria (a type of Lycopod) tree remains in the ceilings of coal mines in the Upper Freeport (UF) and Lewiston-Stockton (LS) seams. Samples were crushed in an adjustable plate mill to reduce the topsize to nominally 2mm, then comminuted in a (Holmes 501XLS) pul-

[†] Accepted : June 25, 2007

¹ 126 Hosler Building, University Park PA 16802, USA

² Norfolk, VA 23529, USA

* Corresponding author

TEL : +814 235 7359

E-mail: jmathews@psu.edu

verizer. Particle were separated by wet sieving. The mean maximum vitrinite reflectance was determined by the ASTM procedure¹⁴. For shape analysis, polished pellets were prepared using a modified ASTM method. Approximately 0.5g of vitrinite was mixed with epoxy in a small vial, centrifuged to remove air bubbles and placed in a vacuum oven to aid epoxy impregnation. After setting, the vial was removed and the sample cut in half lengthways. The sample was cast in a standard optical microscopy pellet and polished. Size and shape analyses were performed using a digital image analysis system (IMAGIST, PGT, Princeton, NJ) interfaced with a (Nikon Microphot-FXA) microscope and a workstation. Oil-immersion objective lenses of 20×, 40× and 100× magnifications were used for 100×200, 200×400 and -400 mesh (U.S. Standard Sieve) size cuts. Over 500 particles were evaluated in each cut, with approximately 20-30 particles in each micrograph.

Oil-immersion objective lenses were used to increase the contrast between mineral matter and vitrinite particles to aid in excluding mineral matter from the shape analyses. Computational editing of the particle outlines removed any holes in the face of the particle silhouette (emanating from mineral matter removal during polishing or from optics contamination). Particle segmentation was used to separate particles that were so closely located as to be erroneously classified as a single particle. Epoxy features, mineral matter (identifiable from reflectance levels), scratched particles, incorrectly segmented particles, particles with greater than 5% of the perimeter off the field of view, and particles with outlines altered by mineral matter inclusions were excluded from the analysis (based on a comparison between the image captured digital silhouette view and microscopy observations). More than 500 particles were analyzed for size and shape in each size cut.

The particle size distributions were also determined by laser light scattering (Malvern Instruments). A monochromatic collimated beam of light was passed through a sample cell containing the sample (several mg) in an ethanol medium with agitation supplied by a spinning bar magnet. The scattered light was brought to focus at the detector and the particle size distribution calculated assuming spherical particles. The assumption of spherical particles is commonly applied in coal science, despite the knowledge that coal particles are not spherical. The lack of quantified shape parameters hinders a more accurate description. To enable the impact of mineral matter to be determined, one sample was demineralized by

treatment with 10% HCl overnight followed by concentrated 52% HF for 100 hours with occasional stirring. Any remaining fine clays were removed with the aid of a dispersant. Following demineralization the samples were washed thoroughly with distilled water and air-dried.

3. Results & Discussion

Maceral identification confirmed the vitrain samples collected from obvious coalified trees were monomaceral (telocollinite) in composition. The mean maximum vitrinite reflectance values were 0.97 (sd 0.04) and 0.93 (sd 0.08) for the UF and LS samples, respectively. These reflectance levels indicate the samples were high volatile bituminous A in rank. Particle diameters were measured with an optical microscope approach and via laser light scattering. Image analysis of micrographs was used to determine individual particle diameters from the average of 12 diameters separated by 15°. The elongation ratio was defined as the smallest of the ratios obtained from these diameters to its perpendicular diameter (the width and the breadth in rectangles.) The aspect ratio was defined as the reciprocal of the elongation ratio. Circularity (O) was calculated from the largest diameter of the particle (d_m) and the particle area using Equation 1. The area (A) was determined from the number of (calibrated) pixels in the particle silhouette. A sphere has a circularity of unity and elongated shapes have higher values.

$$\text{Circularity } O = (d_m)^2(\pi) / (4A) \quad (1)$$

An example of the particle shapes observed from a polished surface of a pellet is presented in **Fig. 1**. The unnumbered features were excluded from the analysis based on the exclusion criteria discussed earlier. The 12 diameters are drawn manually on the particle labeled number 5 to illustrate diameter placement. The size and shape parameters of the numbered particles are listed in **Table 1** to illustrate the relationship between shape and numerical characterization of the shape. As the field of view is from a polished surface, the particles are expected to have different orientations or may expose only a portion of the particle.

As indicated in **Table 1** and **Fig. 1** the UF vitrinite had a variety of shapes. Particle size (determined by microscopy and by light scattering) and shape parameters (determined by microscopy) are shown in **Table 2** for various size cuts. The laser light scat-

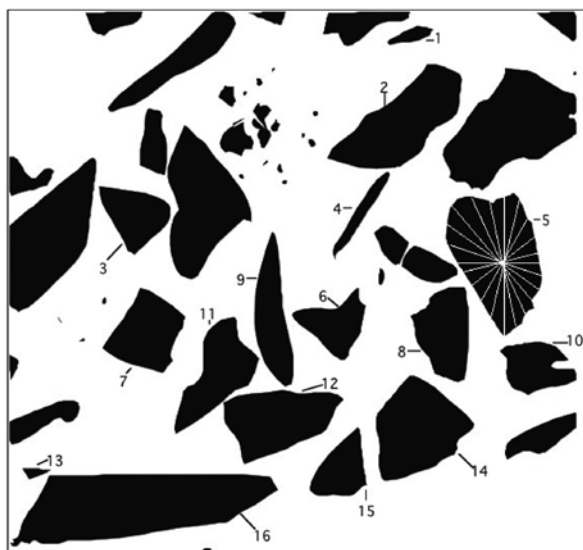


Fig. 1 Silhouette Image of Polished Face the UF 200 × 400 Cut Embedded in Resin.

tering technique measures particle diameters using a median volume-weighted diameter ($D[v,50]$). The microscopy technique measures the median length-weighted diameter ($D[l,50]$). The average aspect ratios were 1.66 and 1.64 for the UF and LS vitrinites, respectively. For the UF size cuts the average aspect ratio and circularity decreased slightly with decreasing particle size cut, indicating that the smaller particles were slightly less elongated. The -400 mesh (US Standard Sieve) cut had an average circularity of 2.36 (**Table 2**), indicating significant non-sphericity (see examples in **Fig. 1** and **Table 1**). There was little change in the average shape parameters among the size cuts and the LS and UF samples had similar values for the same size cut. In contrast to the vitrinite particles, the highly reflecting mineral matter

Table 1. Size and Shape Parameters for UF 200x400 Mesh Size Cut Shown in Fig. 1

| Particle Number | Mean Diameter, μm | Circularity O | Elongation Ratio | Aspect Ratio |
|-----------------|------------------------------|---------------|------------------|--------------|
| 1 | 27.3 | 3.21 | 0.37 | 2.70 |
| 2 | 102.8 | 2.87 | 0.43 | 2.33 |
| 3 | 61.9 | 1.74 | 0.77 | 1.30 |
| 4 | 58.0 | 7.83 | 0.19 | 5.26 |
| 5 | 105.2 | 1.83 | 0.62 | 1.61 |
| 6 | 61.8 | 1.78 | 0.85 | 1.18 |
| 7 | 70.6 | 1.52 | 0.90 | 1.11 |
| 8 | 69.3 | 1.74 | 0.64 | 1.56 |
| 9 | 91.3 | 4.90 | 0.28 | 3.57 |
| 10 | 57.5 | 2.08 | 0.65 | 1.54 |
| 11 | 85.5 | 2.94 | 0.50 | 2.00 |
| 12 | 89.5 | 2.11 | 0.55 | 1.82 |
| 13 | 16.1 | 2.83 | 0.43 | 2.33 |
| 14 | 87.0 | 1.42 | 0.82 | 1.22 |
| 15 | 56.8 | 2.07 | 0.64 | 1.56 |
| 16 | 169.6 | 4.64 | 0.27 | 3.70 |

particles were almost spherical, in agreement with previous observations¹⁵.

There was good agreement between the length-weighted diameters (microscopy) and the volume-weighted diameters (light scattering) for the smaller size cuts (**Table 2**). This is unexpected, as the volumetric weighted diameter is an indication that 50 % of the total volume of the particles is in particles of greater diameter, while the length-weighted diameter indicates that 50 % of the total length of the particles is in those particles of greater diameter. Thus, larger particle sizes contribute disproportionately to the volume-weighted diameter than to the length-weighted diameter. For the LS 200 × 400 cut the volume-weight-

Table 2. Size and Shape Parameters for UF and LS Vitrinite Size Cuts

| Sample | $D[v,50]/\mu\text{m}$ | $D[l,50]/\mu\text{m}$ | Circularity O | Elongation Ratio | Aspect Ratio |
|---------------|-----------------------|-----------------------|---------------|------------------|--------------|
| UF100 × 200 | 131 | 77 (40) | 2.57 (1.09) | 0.57 (0.18) | 1.75 (0.77) |
| UF200 × 400 | 65 | 66 (37) | 2.47 (0.96) | 0.59 (0.17) | 1.69 (0.69) |
| UF200 × 400 ‡ | 63 | | | | |
| UF-400 | 26 | 25 (29) | 2.36 (0.90) | 0.65 (0.16) | 1.54 (0.59) |
| LS100 × 200 | 102 | 82 (40) | 2.48 (0.97) | 0.60 (0.16) | 1.67 (0.64) |
| LS200 × 400 | 61 | 73 | 2.49 | 0.58 | 1.72 |
| LS-400 | 20 | 24 (26) | 2.30 (0.81) | 0.66 (0.16) | 1.52 (0.54) |

$D[l,50]$ is the length weighted mean diameter. $D[v,50]$ is the volumetric weighted average diameter. Other parameters as defined in the text. Values in parentheses are standard deviations.

‡ demineralized sample.

ed (light scattering), surface-weighted (calculated), and length-weighted (calculated) median diameters were 61, 55, and 47 μm , respectively. It is not clear why the volume-weighted and length-weighted median diameters agree so well for the smaller size cuts. One possible explanation is the inclusion of discrete particles of mineral matter in the light scattering data, however demineralization did not significantly alter the volume-weighted diameter of the 200 \times 400 UF cut (**Table 2**). The deviation from sphericity contributes to the significant difference between the calculated (47 μm from light scattering) and measured (73 μm from microscopy) length-weighted diameters for the LS 200 \times 400 cut.

To establish the shape of the coal particles, it was necessary to obtain information on the third dimension. An SEM micrograph conveniently permitted an estimation of the depth of the particle. From **Fig. 2** and other micrographs (not shown), it was concluded that the depth was of the same magnitude as the width. The shape was generally “blocky” with angular transitions. Thus, as a first approximation, the particle can be represented by a square-ended rectangular brick of length and width a and depth $b = a/1.7$ as shown is in **Fig. 3**.

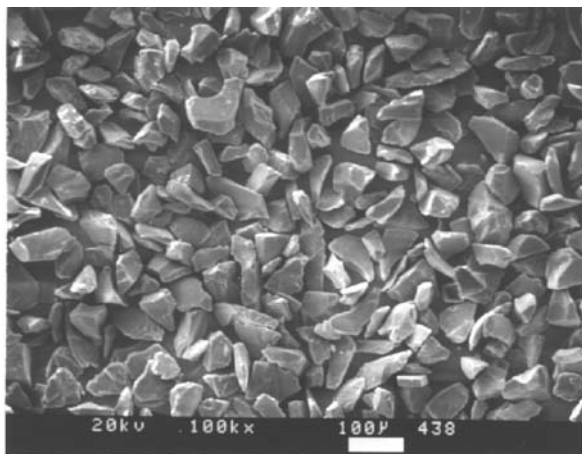


Fig. 2. SEM Micrograph of the UF 200 \times 400 Cut.

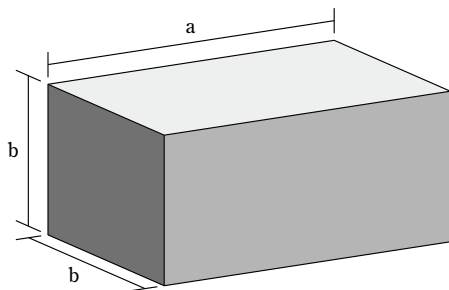


Fig. 3. Shape Descriptors for a Square-Ended House Brick Shape.

Assuming that a vitrinite particle is adequately represented by a square-ended rectangular brick, then equating the diameter of a sphere (d_p), of the same volume as the brick, to the length (a) and width ($b=1/1.7$) yields equation 2.

$$Vol = \frac{a^3}{b^2} = \frac{\pi d_p^3}{6} \text{ or } d_p = 0.87a \quad (2)$$

Sphericity (ϕ_s), the ratio of the surface area of a sphere to the surface area of the particle (of the same volume), yields equation 3, and substituting for d_p in equation 3

$$\phi_s = \frac{\pi d_p^3}{\left(\frac{2}{b^2} + \frac{4}{b}\right) a^2} \quad (3)$$

yields a sphericity ϕ_s of 0.78. Constant sphericity values of 0.73 for pulverized coal dusts have been reported^{16, 17} based on microscopic and sieve analysis of 80, 65 and 50 % of the particles passing 200 mesh British Standard sieve¹⁸. A sphericity of 0.38 has also been reported for fusain fibers^{16, 17}. Unfortunately the coal classification was not reported with these data. A consistent shape factor (using surface areas as determined by liquid permeability and sieve sizes) has also been reported for various size cuts (11 fractions between 16 to 325 US mesh), although particle shape was found to be rank dependent⁵. Aspect ratios of 1.39 to 1.55 have been determined for Pittsburgh seam coal dusts (less than 75 μm diameter) generated within the mine and by a variety of pulverizers⁴. These aspect ratios are consistent with those reported here for the smallest particle size cuts.

When coals are comminuted, the particles break first at the weakest junctures, which are the organic-inorganic, maceral-macerals interfaces and along the pores¹⁹. Thus, at least initially, macerals tend to retain their characteristic shape¹⁹. Macerals also concentrate in different size fractions because of the different friabilities and/or heterogeneity among maceral groups⁶⁻¹¹. Thus, coals are expected to have different shape parameters in different size fractions. With increasing pulverization residence time (of an hour or more), however, the shapes of the particles are altered towards more spherical or “blocky type” shapes¹⁹. Also, there is evidence that different methods of pulverization produce different particle shapes^{4, 5, 20}, although one study found little influence of pulverizer type upon shape²¹. Extended comminution time has also been shown to influence particle shape²⁰ for most of the devices used, the exception

was a high-energy mill. Lithotypes also have different friabilities, with the monomaceral microlithotypes of vitrinite and inertinite being the easiest to grind under Hardgrove grindability conditions, thus, increasing the concentration of trimaceral lithotypes in the coarser grinds²². Caution must therefore be exercised in comparing the results of different studies, as rank, maceral content and pulverization method influence the shape^{4,5}.

Having established the deviation from a sphere, the question arises: what is the impact? As stated earlier, the size and shape of coal particles influence their heat and mass transfer characteristics, behavior in fluids, erosion characteristics and inhalation-related health risks^{1,4}. A simple heat transfer calculation will show if the impact is significant on convective heating where spheres are commonly assumed. Equation 4 shows the commonly used convective heat transfer calculation, Nu is the Nusselt Number (a dimensionless heat transfer coefficient), λ is the thermal conductivity of the gas, and T_g and T_p are the temperature of the gas and particle, respectively.

$$\frac{dQ}{dt} = \frac{Nu\lambda}{d_p} (T_g - T_p) \frac{\pi d_p^2}{\Phi_s} \quad (4)$$

The sphericity is used as a corrective term for non-spherical particles. Addition of the energy gradient term in equation 4 yields equation 5, where C_p is the specific heat of the particle and ρ_p is the particle density. Rearrangement of equation 5 generates equation 6.

$$\pi d_p^3 \rho_p C_p \frac{dT_p}{dt} = \frac{Nu\lambda}{d_p} (T_g - T_p) \pi \frac{d_p^2}{\Phi_s} \quad (5)$$

$$\frac{dT_p}{dt} = \frac{6Nu\lambda}{d_p^2 \Phi_s \rho_p C_p} (T_g - T_p) \quad (6)$$

Defining a characteristic heating time (τ) enables simplification and calculation of the role of sphericity in the heating time. The characteristic heating time is shown in equation 7.

$$\tau = \frac{d_p^2 \Phi_s \rho_p C_p}{6Nu\lambda} \quad (7)$$

Making the assumption that the Nusselt Number is 2 and that the sphericity $\phi_s=0.78$, then τ becomes 22% greater than in the case of a sphere. A more accurate comparison would include the influence of the house brick shape on the characteristic length

component of the Nusselt Number. While this is potentially a significant decrease in effective particle heating rate it is important to note that under rapid heating conditions, occurring during pulverized coal combustion, that most bituminous coals will deform and alter shape. In earlier work these samples were exposed to rapid-heating pyrolysis in a drop-tube reactor²³. A range of time-temperature histories was predicted for particles, depending on path and proximity to the hot walls, utilizing computational fluid dynamics. SEM observations showed that at center line gas temperatures around 841 K (approximately 0.06 s residence time) that rounding of sharp edges was evident in some particles and the occasional particle had formed a swollen spherical particle with an empty interior, known as a cenosphere²⁴, however most particles were unchanged²³. At around 1,000 K center line gas temperatures (0.15-0.17 s center line residence times for UF and LS particles, respectively) many spheres were evident with slightly larger size than the raw feed (a 10-15 μm increase in $D[v,0.5]$)²³. By 1600 K gas temperature and 0.2-0.3 s residence time spectacular swelling (tripling in $D[v,0.5]$ in comparison to the feed) was observed for UF with large cenospheres dominating the particle distribution²³. The LS sample doubled in size on average²³. Particle size influences the heating rate and release of volatiles²⁵, it is demonstrated that the shape influence heating rate and is thus expected to influence volatile transport within the particle and influence thermo-plastic behavior and hence char physical and chemical structure²⁶.

To determine the impact of this shape factor on terminal velocity, a petroleum-based modeling material was weighed and shaped into 3 spheres and 3 appropriately sized square ended rectangular bricks. The same mass was used in each sample. The samples were placed in oil and dropped one at a time into a graduated cylinder filled with the same viscous oil. Time measurements and velocity calculations (timing occurred after terminal velocity had been reached) indicated the sphere fell slower than the orientated house brick shaped samples, 4.0 (± 0.2 s.d.) versus 4.8 (± 0.3) seconds for the sphere. Essentially, the velocity of the square ended brick shape, of the same mass, was 20% faster than the sphere. Time measurements showed random scatter implying the samples did not gain mass after exposure to oil. Thus aerodynamic calculations assuming spheres (of the same mass) will overestimate the suspension of particles in the air or coal-water slurry suspensions.

4. Conclusion

The shapes of two pulverized vitrinite samples in the bituminous rank range were found to be similar among and between the size cuts, in agreement with previous work. A slight decrease in aspect ratio and a slight increase in circularity accompanied decreasing particle size. The -400 mesh US Standard Sieve size cut for each vitrinite had the lowest aspect ratio and the lowest circularity value. The particles had a distribution of shapes but the average particle was approximately 1.7 times as long as it was broad. It was concluded that on average a square-ended rectangular block (house brick shape) of length a and depth and width of $b=a/1.7$ was a more realistic representation of a vitrinite particle than a sphere of the same volume. The two bituminous coals and different size cuts of each coal had essentially the same shape parameters. A sphericity value of 0.78 was determined for the pulverized bituminous vitrinites in agreement with a previously reported value of 0.73 for coals in general. Characteristic heating times and terminal velocities were higher by 22 and 20%, respectively compared to spherical particles.

Acknowledgements

The authors thank Dr. Peter Walsh currently at The University of Alabama at Birmingham for assistance in the heat transfer calculation.

Symbols

| | | |
|-----------|---|--------------------|
| A | particle area | $[m^2]$ |
| a | particle width | $[m]$ |
| b | particle breadth | $[m]$ |
| Cp | specific heat of the particle | $[JK^{-1}kg^{-1}]$ |
| $D[l,50]$ | median length-weighted diameter | $[m]$ |
| $D[v,50]$ | median volume-weighted diameter | $[m]$ |
| d_m | largest particle diameter from 12 measurements 15° apart | $[m]$ |
| LS | Lewiston Stockton seam coal sample | $[-]$ |
| Nu | Nusselt Number | $[-]$ |
| ρ_p | particle density | $[kgm^{-3}]$ |
| O | circularity | $[-]$ |
| Q | heat | $[J]$ |
| τ | characteristic heating time | $[S]$ |
| T_g | temperature of the gas | $[K]$ |
| T_p | temperature of the particle | $[K]$ |
| UF | Upper Freeport coal seam sample | $[-]$ |
| vol | particle volume | $[m^3]$ |
| π | pi | $[-]$ |

| | | |
|-----------|---------------------------------|-------------------|
| ϕ_s | sphericity | $[-]$ |
| λ | thermal conductivity of the gas | $[Wm^{-1}K^{-1}]$ |

References

- 1) Thakur, P. C.: Mass distribution, percent yield, non-settling size and aerodynamic shape factor of respirable coal dust particles, MS, The Pennsylvania State University, University Park, PA (1971).
- 2) Raask, E.: Erosion ware in coal utilization, Washington, DC, Hemisphere (1988).
- 3) Dumm, T. F.: Characterization of size/composition and shape of fine coal and mineral particles, PhD., The Pennsylvania State University, University Park, PA (1989).
- 4) Li, J.: Size shape and chemical characteristics of mining generated and laboratory-generated coal dusts, MS, The Pennsylvania State University, University Park, PA (1990).
- 5) Austin, L. G., R. P. Gardner and P. L. Walker: "The shape factors of coals ground in a standard Hardgrove mill", *Fuel*, 42, (2), 319 (1963).
- 6) Davis, A. and P. C. Orban, Size segregation of component coals during pulverization of high volatile/low volatile blends, *Twelfth Annual International Pittsburgh Coal Conference*, Univ. of Pittsburgh, 312 (1995).
- 7) Jones, R. B., C. B. McCourt, C. Morley and K. King: "Maceral and rank influences on the morphology of coal char", *Fuel*, 64, (10), 1460 (1985).
- 8) Arnold, B. J. and D. B. Smith: "Coal blending-meeting specifications", *Mining Engineering*, 10, 1144 (1994).
- 9) Gibbins, J. R., J. Jacobs, C. K. Man and K. J. Pendlebury, Effect of coal particle size on volatile yields during rapid heating, *Am. Chem. Soc. Div. Fuel Chem. Prepr.*, Washington, D. C., 37, 4, 1930 (1992).
- 10) Palmer, A. D., M. Cheng, J.-C. Goulet and E. Furimsky: "Relation between particle size and properties of some bituminous coals", *Fuel*, 69, (2), 183 (1990).
- 11) Stach, E., M.-T. Mackowsky, M. Teichmuller, G. H. Taylor, D. Chandra and R. Teichmuller: *Coal Petrology*, Berlin, Germany, Gebrueder Borntraeger (1982).
- 12) Taulbee, D., S. H. Poe, T. Robl and B. Keogh: "Density gradient centrifugation separation and characterization of maceral groups from a mixed maceral bituminous coal", *Energy & Fuels*, 3, 662 (1989).
- 13) ASTM: Designation: D2799-05a, Standard Test Method for Microscopical Determination of Volume Percent of Physical Components of Coal, in Annual book of ASTM standards, Section 5, Petroleum products, lubricants and fossil fuels, (2006).
- 14) ASTM: Standard test method for microscopical determination of the reflectance of vitrinite in a polished specimen of coal, in Annual book of ASTM standards, Section 5, Petroleum products, lubricants and fossil fuels, 274 (1995).
- 15) Lin, J. S., R. W. Hendricks, L. A. Harris and C. S. Yust: "Microporosity and micromineralogy of vitrinite in a

- bituminous coal”, *J. Appl. Cryst.*, 11, 621 (1978).
- 16) Sakiadis, B. C.: Fluid and Particle Mechanics, in Perry’s Chemical Engineer’s Handbook, Perry, R. G. and Green, D., McGraw, New York, Chapter 5 (1984).
 - 17) Carman, P. C.: “Fluid flow through granular beds”, *Trans. Inst. Chem. Eng. (London)*, 15, 150 (1937).
 - 18) Heywood, H.: “Calculating the specific surface of a powder”, *I. Mech E.*, 125, 383 (1933).
 - 19) Lytle, J. M., J. L. Daniel and K. A. Prisbrey: “Effect of microstructure on the size and shape of coal particles during comminution”, *Fuel*, 62, (11), 1304 (1983).
 - 20) Kaya, E., R. Hogg and S. R. Kumar: “Particle shape modification in comminution”, *KONA*, 20, 188 (2002).
 - 21) Heywood, H.: “Characteristics of pulverised fuels”, *The Inst. of Fuel*, 6, 241 (1933).
 - 22) Hower, J. C. and G. D. Wild: “Maceral / microlithotype analysis evaluation of coal grinding: examples from central Appalachian high volatile bituminous coals”, *Journal of Coal Quality*, 13, (2), 35 (1994).
 - 23) Mathews, J. P., P. G. Hatcher, S. Eser, P. Walsh and A. W. Scaroni, Time-temperature histories of bituminous coal particles in a drop-tube reactor, *Prepr. Am. Chem. Soc., Div Fuel Chem.*, Boston, MA, August 22-27, 1998, 43, 3, 611 (1998).
 - 24) Newall, H. E. and F. S. Sinatt: “The carbonization of coal in the form of fine particles. I. The production of cenospheres”, *Fuel*, 3, 424 (1924).
 - 25) Griffin, T. P., J. B. Howard and W. A. Peters: “An experimental and modeling study of heating rate and particle size effects during pyrolysis”, *Energy & Fuels*, 7, (2), 297 (1993).
 - 26) Grey, V. R.: “The role of explosive ejection in the pyrolysis of coal”, *Fuel*, 67, (9), 1298 (1988).

Author’s short biography



Jonathan Mathews

Jonathan Mathews is a coal scientist. He holds an honors degree in Applied Chemistry (1991) from the Nottingham-Trent University in Britain and a doctorate in Fuel Science (1998) from the Pennsylvania State University. He is an assistant professor in the Energy & Mineral Engineering Department, College of Earth & Mineral Sciences, at the Pennsylvania State University. His research is focused on the structure of coal and structural influences upon coal behavior. His focus spans the molecular scale with molecular modeling simulation, micron scale with advanced image analysis, and larger scales with X-ray computed tomography among other techniques. Currently his focus is on sequestration of CO₂ in coal.



Dr. Semih Eser

Semih Eser is an Associate Professor of Energy and Mineral Engineering. Eser received his B.S. (1976) and M.S. (1978) degrees in Chemical Engineering from Middle East Technical University in Ankara, Turkey and his Ph.D. (1986) in Fuel Science from Penn State University. From 1987 to 1988, he worked as a research associate in the Department of Chemical Engineering at Auburn University. He returned to Penn State in 1988 and was appointed as an assistant professor of Fuel Science in 1989. He served the Department of Energy and Geo-Environmental Engineering as Associate Head (2001-2006) and Acting Head (2004). He served the Penn State Energy Institute as the associate director and director of the Laboratory for Hydrocarbon Process Chemistry (1995-200), and, currently, he coordinates research on carbon materials at the Institute. His research interests include the reactivity and microscopic characterization of cokes and carbons, coke/carbon formation and deposition mechanisms, inhibition of undesired carbon deposition, and molecular analysis and processing of petroleum feedstocks. His professional activities include serving as Program Chair (2004) and Chair (2006) in the Fuel Chemistry Division of American Chemical Society, and currently serving on the editorial boards of the Journal of ASTM International, Chemistry Central Journal, and Journal of Oil, Gas, and Coal Technology.

Author's short biography



Dr. Patrick G. Hatcher

Patrick G. Hatcher obtained his Ph.D. in chemistry (geochemistry) from the University of Maryland in 1980 after having obtained a MS degree in chemical oceanography from the University of Miami (1974) and a BS degree in chemistry from N.C. State University (1970). He then was employed by the U.S. Geological Survey and later accepted a position at Penn State University. From his eventual position as a Professor of Fuel Science and Geosciences, Adjunct Professor of Chemistry, and Director of The Center for Environmental Chemistry and Geochemistry at Penn State, Hatcher joined the Department of Chemistry at The Ohio State University in July, 1998 and assumed the Directorship of the Ohio State Environmental Molecular Science Institute. In 2006, Hatcher accepted the Batten Endowed Chair of Physical Sciences in the Department of Chemistry and Biochemistry at Old Dominion University and is the Faculty Director of the College of Sciences Major Instrumentation Cluster (COSMIC). He is the author of more than 250 peer-reviewed articles that report on the numerous studies in the area of environmental chemistry and geochemistry, specifically emphasizing the origin, structure, and chemical transformations of plant-derived biopolymers in soils, peats, coals, marine sediments, and oceanic waters. Hatcher relies on modern analytical methods that include 1-,2-, and 3-D liquids NMR as well as solids NMR and electrospray ionization with ultrahigh resolution mass spectrometry.



Dr. Alan W. Scaroni

Alan Scaroni is Associate Dean for Graduate Education and Research and Professor of Energy and Mineral Engineering in the College of Earth and Mineral Sciences at The Pennsylvania State University. He received his bachelor's degree in chemical engineering in 1974 from the University of New South Wales, Australia and M.S. (1979) and Ph.D. (1981) degrees in fuel science from Penn State. His research is focused on controlling emissions from energy systems, both stationary and mobile.